JACS
JOURNAL OF THE AMERICAN CHEMICAL SOCIETY

Communication

pubs.acs.org/JACS

Intense Chiroptical Switching in a Dicationic Helicene-Like Derivative: Exploration of a Viologen-Type Redox Manifold of a Non-Racemic Helquat

Lubomír Pospíšil,*[,†,‡] Lucie Bednárová,*[,†] Petr Štěpánek,[†,§] Petr Slavíček,[∥] Jan Vávra,[†] Magdaléna Hromadová,[‡] Helena Dlouhá,[†] Ján Tarábek,[†] and Filip Teplý*[,†]

[†]Institute of Organic Chemistry and Biochemistry, Academy of Sciences of the Czech Republic, 16610 Prague, Czech Republic
[‡]J. Heyrovský Institute of Physical Chemistry, Academy of Sciences of the Czech Republic, 18223 Prague, Czech Republic
[§]Institute of Physics, Faculty of Mathematics and Physics, Charles University, 12116 Prague, Czech Republic
[∥]Department of Physical Chemistry, Institute of Chemical Technology, 16628 Prague, Czech Republic

Supporting Information

ABSTRACT: Two-step redox switching in enantiopure helquat system $[P\text{-}\mathbf{1}]^{2+} \rightleftharpoons [P\text{-}\mathbf{1}]^{\bullet+} \rightleftharpoons [P\text{-}\mathbf{1}]^{0}$ is demonstrated. The viologen-type electroactive unit embedded directly in the helical scaffold of **1** is responsible for the prominent chiroptical switching at 264 nm. This process is associated with a marked sign-reversal of Cotton effect ramping between $\Delta\varepsilon = +35\ M^{-1}\ cm^{-1}$ for $[P\text{-}\mathbf{1}]^{2+}$ and $\Delta\varepsilon = -100\ M^{-1}\ cm^{-1}$ for $[P\text{-}\mathbf{1}]^{0}$. This helically chiral system features the most intense chiroptical switch response documented in the field of helicenoids.

Helicenes and helicene-like compounds[1] continue to attract attention due to their iconic helical shape, unique chiroptical properties, and their promising potential for the field of catalysis[2] as well as self-assembly.[3] Large chiroptical responses have been recently studied in several helicene-based systems.[4] However, reports on modulation of chiroptical properties of helicenoids by changing their redox state have been surprisingly rare.[5−9] Rajca and Lapkowski groups studied chiroptical properties of configurationally stable thiophene-based [7]helicene **2** and its radical-cation (Scheme 1a).[5] Redox-triggered chiroptical switches based on ruthenium-vinylhelicene **3** and tetrathiafulvalene-helicene conjugate **4** have been investigated by Réau, Crassous, Autschbach et al.[6] and Avarvari, Crassous et al.,[7] respectively (Scheme 1a).

Herein, we report our results on intense two-step chiroptical switching in an enantiopure helquat system $[P\text{-}\mathbf{1}]^{2+} \rightleftharpoons [P\text{-}\mathbf{1}]^{\bullet+} \rightleftharpoons [P\text{-}\mathbf{1}]^{0}$ (Scheme 1b). This helically chiral switch is unique from several perspectives: (1) it represents a chiral electrochemical manifold based on combination of viologen and helicene structural motifs; (2) the viologen-type electroactive unit is inherently integrated in the helix rather than being appended at the periphery of the helical chromophore; (3) our helically chiral system features the most intense chiroptical switch response documented so far in the field of helicenoids ($\Delta(\Delta\varepsilon) = -135\ M^{-1}\ cm^{-1}$ at 264 nm for transition $[P\text{-}\mathbf{1}]^{2+} \rightarrow [P\text{-}\mathbf{1}]^{0}$). To this end, 264 nm is a particularly favorable readout channel as it takes advantage of a remarkable Cotton effect sign-reversal which leads to pronounced switching between $\Delta\varepsilon = +35\ M^{-1}\ cm^{-1}$ for $[P\text{-}\mathbf{1}]^{2+}$ and $\Delta\varepsilon = -100\ M^{-1}\ cm^{-1}$ for $[P\text{-}\mathbf{1}]^{0}$.

Scheme 1. (a) Rare Helicene-Based Chiral Systems 2−4 Where Redox Modulation of the Chiroptical Response Has Been Studied and (b) Chiroptical Switch $[P\text{-}\mathbf{1}]^{2+} \rightleftharpoons [P\text{-}\mathbf{1}]^{\bullet+} \rightleftharpoons [P\text{-}\mathbf{1}]^{0}$ Described in This Work

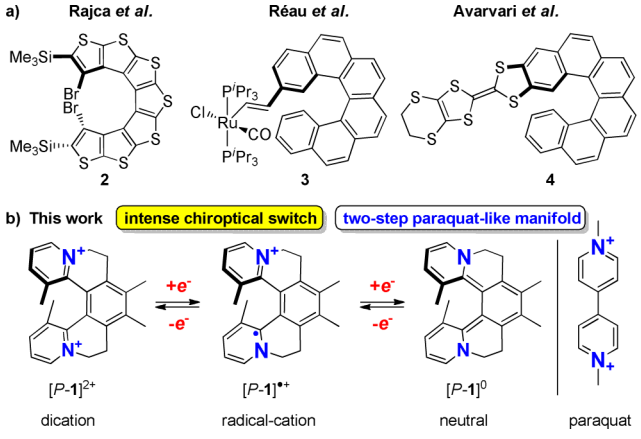

In our recent studies, we introduced helquats,[10] as a new class of helical dications that represent a structural link between helicenes and viologens. Our research is driven by a hypothesis that embedding the dicationic electroactive unit of viologens into the helical scaffold of helicenes will lead to interesting[11] and applicable chemistry. In the course of our investigations of helquats, we recently devised three-step nonchromatographic synthesis of [5]helquat **1**[12] and resolved it to separate enantiomers $[P\text{-}\mathbf{1}]^{2+}$ and $[M\text{-}\mathbf{1}]^{2+}$ in multigram quantities.[12b] Previously, we also examined electron-transfer properties of several racemic helquats including rac-**1**.[13] In the present study, with the enantiopure material available, we set out to examine the redox-triggered modulation of chiroptical properties of the individual enantiomeric forms $[P\text{-}\mathbf{1}]^{2+}$ and $[M\text{-}\mathbf{1}]^{2+}$. To this end, cyclic voltammetry experiment with $[P\text{-}\mathbf{1}]^{2+}$ (Figure 1, inset) was performed first. Two consecutive reversible single-electron-

Received: January 8, 2014
Published: March 5, 2014

 © 2014 American Chemical Society dx.doi.org/10.1021/ja500220j | J. Am. Chem. Soc. 2014, 136, 10826−10829

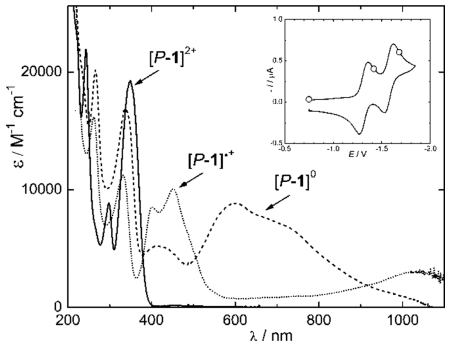

Figure 1. UV−vis absorption spectroelectrochemistry of $[P\text{-}\mathbf{1}]^{2+}$ triflate (acetonitrile/*n*-Bu_4NPF_6). The potential was scanned between −0.7 and −1.8 V, and the spectrum of the oxidized form $[P\text{-}\mathbf{1}]^{2+}$ (full line) is observed for potentials higher than −1.1 V vs Fc/Fc^+. At −1.4 V, spectrum of the radical-cation $[P\text{-}\mathbf{1}]^{\bullet+}$ develops (dotted line). Spectrum of the fully reduced form $[P\text{-}\mathbf{1}]^0$ (dashed line) is obtained at −1.65 V vs Fc/Fc^+, and the potential scan back recovers all the initial spectral features. Inset shows the cyclic voltammogram (CV) starting with $[P\text{-}\mathbf{1}]^{2+}$ triflate (acetonitrile/*n*-Bu_4NPF_6, mercury drop working electrode, scan rate 0.5 V/s). Circles in the CV indicate potentials, where the UV−vis absorption and ECD spectra were measured (−1.4 V, −1.65 V).

transfer steps at half-wave potentials −1.32 and −1.59 V vs the ferrocene/ferrocenium couple (Fc/Fc^+) were observed.

The first electron uptake produces the radical-cation $[P\text{-}\mathbf{1}]^{\bullet+}$ with a signature in the EPR spectrum, and the second electron transfer leads to the fully reduced neutral form $[P\text{-}\mathbf{1}]^0$. The spectral characteristics of both reduced forms of P-**1** are most conveniently measured by in situ methods. A special electrochemical optically transparent thin-layer cell (OTTLE)[14] was directly placed in the optical path, and the spectra were collected during a slow voltage scan. The resulting UV−vis absorption spectra of all three redox forms of $[P\text{-}\mathbf{1}]^{2+}$ are shown in Figure 1.[15] The UV−vis spectrum of $[P\text{-}\mathbf{1}]^{\bullet+}$ recorded at −1.4 V shows a new prominent band at 450 nm, while the spectrum recorded at −1.65 V, which was assigned to the fully reduced form $[P\text{-}\mathbf{1}]^0$, exhibits an intense band at 600 nm with a shoulder at 720 nm. Detailed development of spectral features in the course of redox process and the calculated UV−vis spectra are given in Figures S1 and S2, respectively. This initial UV−vis spectroelectrochemical survey with both enantiomers served for the design of experiments targeted at the redox switching of chiroptical properties.[16] The experimental electronic circular dichroism (ECD) spectra for each enantiomer of species **1** in all three redox states are given in Figure 2. These experiments established that the ECD spectra of $[P\text{-}\mathbf{1}]^{2+}$ and its reduced forms are mirror images of the spectra of the corresponding three redox forms derived from $[M\text{-}\mathbf{1}]^{2+}$. For simplicity, in further discussion we focus only on the redox manifold of **1** having P helicity.

The comparison of ECD spectra between the three redox forms shows remarkable and unprecedented changes of the chiroptical properties (Figure 2). The reduction of $[P\text{-}\mathbf{1}]^{2+}$ to the radical-cation $[P\text{-}\mathbf{1}]^{\bullet+}$ leads to broadening and red shift of two positive ECD bands at 261 and 296 nm by ∼30 nm. At the same time, two negative bands of $[P\text{-}\mathbf{1}]^{2+}$ at 243 and 337 nm are shifted to 261 and 447 nm, respectively. The negative band at 447 nm observed for $[P\text{-}\mathbf{1}]^{\bullet+}$ has a shoulder at 400 nm, and a new feature is a broad positive band around 725 nm. Further reduction $[P\text{-}\mathbf{1}]^{\bullet+} \rightarrow [P\text{-}\mathbf{1}]^0$ also results in pronounced effects. Specifically, the ECD spectrum of $[P\text{-}\mathbf{1}]^0$ exhibits two distinct positive bands at 344 and 558 nm of comparable intensity and two negative bands at 264 and 712 nm. The long wavelength bands (558 and 712 nm) were both absent in the ECD spectrum of the original form $[P\text{-}\mathbf{1}]^{2+}$.

The electrochemical reversibility mentioned above prompted us to explore the chiroptical switching triggered by the applied potential steps. Values of the individual potentials suitable for ECD switching were selected according to the current−voltage curve shown in the inset of Figure 1, whereas the selection of wavelengths was based on inspection of ECD spectra of each redox form of P-**1** (Figures 2 and S3). The cycling of potential steps between reduction(s) and oxidation(s) causes either marked change of the sign of ECD from positive to negative values (Figure 3A,E) or an ON/OFF switching of the ECD signal (Figure 3C). Notably, ECD signal at 282 nm can be switched gradually in two separate potential steps directly visualizing the presence of all three redox forms of P-**1** in the switching process (Figure 3E). The ECD switching is accompanied by changes of the UV−vis absorbance (Figures 3B,D,F and Table S1 for *g*-factor values).

Stepwise changes of UV−vis absorption and ECD spectra co-occur with EPR signal switching. This is shown in experiments, in which the potential steps were applied to the spectroelectrochemical cell placed in the cavity of EPR spectrometer (Figures 4, S6, and S7).[17] The hyperfine structure of the $[P\text{-}\mathbf{1}]^{\bullet+}$ EPR spectrum (g^{exp} = 2.00282, see SI, page S13) could not be resolved even by intensive spectral accumulation and applying low-magnetic field modulation amplitudes (down to 0.005 mT at

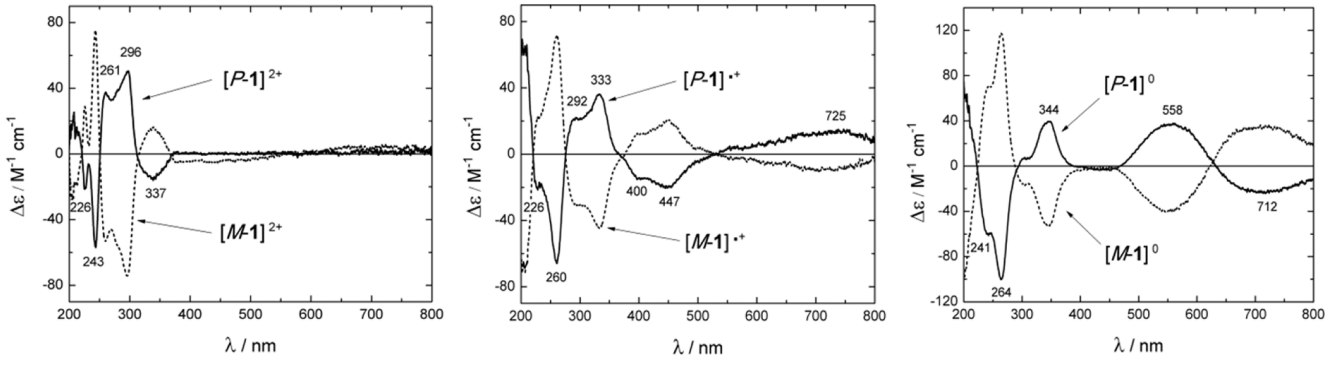

Figure 2. ECD spectrum of 1.95 mM $[P\text{-}\mathbf{1}]^{2+}$ triflate in acetonitrile/0.2 M *n*-Bu_4NPF_6 (left panel, full line). The middle panel shows ECD spectrum of the corresponding radical-cation $[P\text{-}\mathbf{1}]^{\bullet+}$, and the spectrum in the right panel corresponds to the fully reduced neutral form $[P\text{-}\mathbf{1}]^0$. ECD spectra of $[M\text{-}\mathbf{1}]^{2+}$ and its reduced products $[M\text{-}\mathbf{1}]^{\bullet+}$, $[M\text{-}\mathbf{1}]^0$ are given by dashed lines. Key ECD maxima and minima of $[P\text{-}\mathbf{1}]^{2+}$, $[P\text{-}\mathbf{1}]^{\bullet+}$, and $[P\text{-}\mathbf{1}]^0$ are annotated with wavelengths given as numbers next to the corresponding bands.

dx.doi.org/10.1021/ja500220j | J. Am. Chem. Soc. 2014, 136, 10826−10829

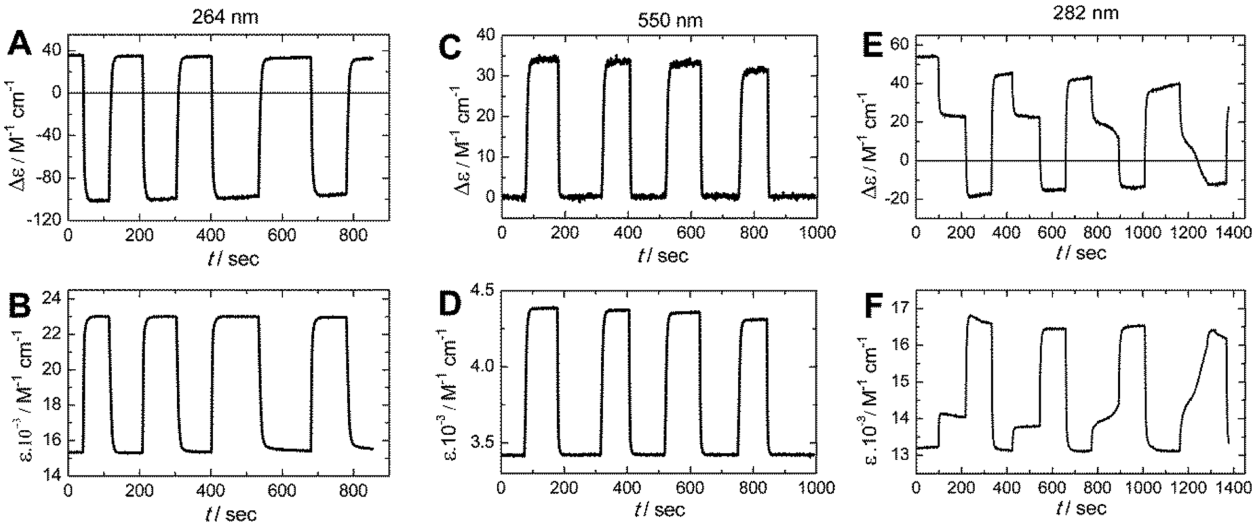

Figure 3. Redox switching of ECD response (A, C, and E) and the corresponding changes in UV−vis absorption (B, D, and F) at selected wavelengths (indicated above the top panels). Panels A−D show switching results after application of potential steps between the oxidation and the full reduction $[P\text{-}\mathbf{1}]^{2+}/[P\text{-}\mathbf{1}]^{0}$. Gradual ramping of potentials between the three species $[P\text{-}\mathbf{1}]^{2+}$, $[P\text{-}\mathbf{1}]^{\bullet+}$, and $[P\text{-}\mathbf{1}]^{0}$ leads to optical changes displayed in panels E and F. The solution composition was the same as in Figure 2.

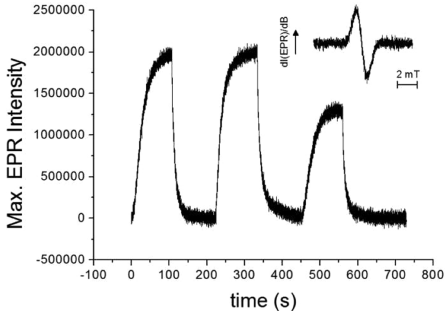

Figure 4. Switching of the EPR signal in the $[P\text{-}\mathbf{1}]^{2+}/[P\text{-}\mathbf{1}]^{\bullet+}$ redox manifold by applying potential pulses between −0.3 V and the first reduction step (−1.3 V). Inset: EPR spectrum (reduction of 10^{-3} M $[P\text{-}\mathbf{1}]^{2+}$/acetonitrile/0.2 M n-Bu_4NPF_6).

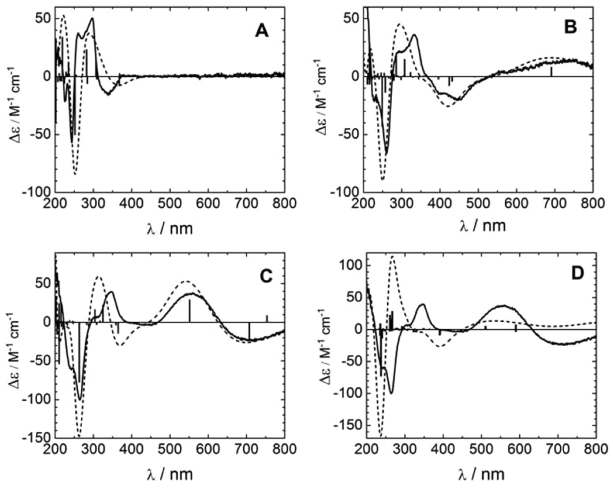

Figure 5. Comparison of experimental ECD spectra (full lines) and calculated spectra (bars and dotted lines): (A) $[P\text{-}\mathbf{1}]^{2+}$, (B) $[P\text{-}\mathbf{1}]^{\bullet+}$, (C) singlet of $[P\text{-}\mathbf{1}]^{0}$, and (D) triplet of $[P\text{-}\mathbf{1}]^{0}$.

100 kHz modulation), indicating that the hyperfine splitting/coupling constants of $[P\text{-}\mathbf{1}]^{\bullet+}$ are rather small. This was corroborated by the DFT calculations using the UB3LYP/EPR-(II)(C,H)/EPR-III(N)/CPCM level of theory which revealed that the highest spin density resides in the terminal heterocyclic moieties of the $[P\text{-}\mathbf{1}]^{\bullet+}$ (see Figure S8 and Table S2).

Further information on identity of the individual species in the redox manifold was obtained from first-principles calculations at B3LYP/TZVP/PCM level (see SI, page S3).[18] The simulated ECD spectra for $[P\text{-}\mathbf{1}]^{2+}$ and $[P\text{-}\mathbf{1}]^{\bullet+}$ reproduce the experimental results well in all major features (Figure 5A,B). Insight into the electronic nature of $[P\text{-}\mathbf{1}]^{0}$, which resembles diradical species such as Thiele's and Chichibabin's hydrocarbons,[19] was obtained from comparison of calculated energies of $[P\text{-}\mathbf{1}]^{0}$ singlet vs $[P\text{-}\mathbf{1}]^{0}$ triplet. This revealed the singlet state to be 38.3 kJ·mol^{-1} lower in energy than the triplet. Moreover, agreement between the experimental and the calculated ECD spectra is better for the singlet species rather than for triplet (Figure 5C vs D), further indicating that the $[P\text{-}\mathbf{1}]^{0}$ is in closed shell singlet state (see SI, page S11).[20]

In summary, we introduced intense redox-triggered chiroptical switching in two-step viologen-type electrochemical manifold $[P\text{-}\mathbf{1}]^{2+} \rightleftharpoons [P\text{-}\mathbf{1}]^{\bullet+} \rightleftharpoons [P\text{-}\mathbf{1}]^{0}$. This helically chiral switch based on an enantiopure [5]helquat is remarkable as it features the most prominent chiroptical switch response documented so far in the field of helicenoids ($\Delta(\Delta\varepsilon) = -135$ M^{-1} cm^{-1} in ECD).[21] The ECD switching at 264 nm is associated with a marked sign-reversal of Cotton effect ramping between $\Delta\varepsilon = +35$ M^{-1} cm^{-1} for $[P\text{-}\mathbf{1}]^{2+}$ and $\Delta\varepsilon = -100$ M^{-1} cm^{-1} for $[P\text{-}\mathbf{1}]^{0}$. Significant chiroptical switching at 550 nm and region around 700 nm bordering with NIR are also notable (Figures 3C and SI, pages S7, S8). To this end, our results show that enantiopure helquats such as $[P\text{-}\mathbf{1}]^{2+}$ can uniquely combine the typical features attributed to the two well-known compound classes, viologens and helicenes,[22] with the former being widely useful in electrochemical applications and the latter having outstanding chiroptical properties. The chiral electrochemical manifold of $[P\text{-}\mathbf{1}]^{2+}$ is due to the viologen-type electroactive unit integrated directly into the helical scaffold rather than being appended at the periphery of the helix. Moreover, the helically chiral switch **1** is readily available in gram quantities in both enantiomeric forms, $[P\text{-}\mathbf{1}]^{2+}$ and $[M\text{-}\mathbf{1}]^{2+}$.[12b] Chiroptical switching materials, such as

dx.doi.org/10.1021/ja500220j | J. Am. Chem. Soc. 2014, 136, 10826−10829

the enantiopure helquat reported herein, are expected to find applications in polarization-related photonics for data storage, optical switches and light modulators[23] and in the emerging field of chiral organic conducting systems.[24]

■ ASSOCIATED CONTENT

Supporting Information

Experimental and computational details. This material is available free of charge via the Internet at http://pubs.acs.org.

■ AUTHOR INFORMATION

Corresponding Authors

lubomir.pospisil@jh-inst.cas.cz
bednarova@uochb.cas.cz
teply@uochb.cas.cz

Notes

The authors declare no competing financial interest.

■ ACKNOWLEDGMENTS

Financial support by the Czech Science Foundation (13-19213S, P.Sl. acknowledges project no. 13-34168S), and the Academy of Sciences of the Czech Republic (RVO: 61388963) is gratefully acknowledged. The access to the CERIT-SC computing facilities provided under the Center CERIT Scientific Cloud, part of the Operational Program Research and Development for Innovations (CZ. 1.05/3.2.00/08.0144) is highly appreciated.

■ REFERENCES

(1) (a) Shen, Y.; Chen, C. F. *Chem. Rev.* **2012**, *112*, 1463. (b) Gingras, M. *Chem. Soc. Rev.* **2013**, *42*, 1051. (c) Stará, I. G.; Starý, I. In *Science of Synthesis*; Siegel, J. S., Tobe, Y., Eds.; Thieme: Stuttgart, 2010, Vol. *45b*, pp 885−953. (d) Rajca, A.; Miyasaka, M. In *Functional Organic Materials*; Müller, T. J. J., Bunz, U. H. F., Eds.; Wiley-VCH: Weinheim, 2007, pp 543−577. (e) Urbano, A. *Angew. Chem., Int. Ed.* **2003**, *42*, 3986. (f) Katz, T. J. *Angew. Chem., Int. Ed.* **2000**, *39*, 1921. (g) Collins, S. K.; Vachon, M. P. *Org. Biomol. Chem.* **2006**, *4*, 2518. Aza- and azonia-helicenes: (h) Sato, K.; Arai, S. In *Cyclophane Chemistry for the 21st Century*; Takemura, H., Ed.; Research Signpost: Trivandrum, 2002, pp 173−197. (i) Dumitrascu, F.; Dumitrescu, D. G.; Aron, I. *Arkivoc* **2010**, 1. (i) (j) Arai, S.; Yafune, T.; Ohkubo, M.; Hida, M. *Tetrahedron Lett.* **1989**, *30*, 7217. (k) Torricelli, F.; Bosson, J.; Besnard, C.; Chekini, M.; Bürgi, T.; Lacour, J. *Angew. Chem., Int. Ed.* **2013**, *52*, 1796.

(2) (a) Peng, Z.; et al. *Chem. Rec.* **2013**, *13*, 28. (b) Yavari, K.; et al. *Angew. Chem., Int. Ed.* **2014**, *53*, 861 and refs therein.

(3) (a) Fasel, R.; et al. *Nature* **2006**, *439*, 449. (b) Verbiest, T.; et al. *Science* **1998**, *282*, 913. (c) Kaseyama, T.; et al. *Angew. Chem., Int. Ed.* **2011**, *50*, 3684. (d) Rahe, P.; et al. *J. Phys. Chem. C* **2010**, *114*, 1547.

(4) (a) Anger, E.; et al. *J. Am. Chem. Soc.* **2011**, *133*, 3800. (b) Norel, L.; et al. *Angew. Chem., Int. Ed.* **2010**, *49*, 99. (c) Graule, S.; et al. *J. Am. Chem. Soc.* **2009**, *131*, 3183. (d) Miyasaka, M.; et al. *Angew. Chem., Int. Ed.* **2009**, *48*, 5954. (e) Roose, J.; et al. *Eur. J. Org. Chem.* **2013**, 3223. (f) Wigglesworth, T. J.; et al. *J. Am. Chem. Soc.* **2005**, *127*, 7272.

(5) Zak, J. K.; Miyasaka, M.; Rajca, S.; Lapkowski, M.; Rajca, A. *J. Am. Chem. Soc.* **2010**, *132*, 3246.

(6) Anger, E.; Srebro, M.; Vanthuyne, N.; Toupet, L.; Rigaut, S.; Roussel, C.; Autschbach, J.; Crassous, J.; Réau, R. *J. Am. Chem. Soc.* **2012**, *134*, 15628.

(7) Biet, T.; Fihey, A.; Cauchy, T.; Vanthuyne, N.; Roussel, C.; Crassous, J.; Avarvari, N. *Chem.—Eur. J.* **2013**, *19*, 13160.

(8) (a) Nishida, J.; Suzuki, T.; Ohkita, M.; Tsuji, T. *Angew. Chem., Int. Ed.* **2001**, *40*, 3251. (b) Wang, Z. Y.; Todd, E. K.; Meng, X. S.; Gao, J. P. *J. Am. Chem. Soc.* **2005**, *127*, 11552. (c) Ueda, A.; Wasa, H.; Suzuki, S.; Okada, K.; Sato, K.; Takui, T.; Morita, Y. *Angew. Chem., Int. Ed.* **2012**, *51*, 6691.

(9) For reviews on chiroptical switches: (a) Canary, J. W. *Chem. Soc. Rev.* **2009**, *38*, 747. (b) *Molecular Switches*, 2nd ed.; Feringa, B. L., Browne, W. R., Eds.; Wiley-VCH: Weinheim, 2011; Vol. *1*, pp 121−180. (c) *Comprehensive Chiroptical Spectroscopy*; Berova, N., Polavarapu, P. L., Nakanishi, K., Woody, R. W., Eds.; Wiley: Hoboken, NJ, 2012; Vol. *2*. (d) Wolf, C., Ed. *Dynamic Stereochemistry of Chiral Compounds*; RSC Publishing: Cambridge, 2008.

(10) (a) Adriaenssens, L.; et al. *Chem.—Eur. J.* **2009**, *15*, 1072. (b) Severa, L.; et al. *Tetrahedron* **2010**, *66*, 3537. (c) Vávra, J.; et al. *J. Org. Chem.* **2013**, *78*, 1329.

(11) (a) Adriaenssens, L.; et al. *Chem. Sci.* **2011**, *2*, 2314. (b) Severa, L.; et al. *Angew. Chem., Int. Ed.* **2012**, *51*, 11972. (c) Shaffer, C. J.; et al. *Angew. Chem., Int. Ed.* **2012**, *51*, 10050. (d) Balogh, D.; et al. *Nano Lett.* **2012**, *12*, 5835.

(12) (a) Severa, L.; et al. *New J. Chem.* **2010**, *34*, 1063. (b) Vávra, J.; et al. *Eur. J. Org. Chem.* **2012**, 489.

(13) Pospíšil, L.; et al. *Phys. Chem. Chem. Phys.* **2010**, *12*, 1550.

(14) Krejčík, M.; Daněk, M.; Hartl, F. *J. Electroanal. Chem.* **1991**, *317*, 179.

(15) UV−vis spectra identical to $[P\text{-}\mathbf{1}]^{2+}$ were obtained also for the other enantiomer, $[M\text{-}\mathbf{1}]^{2+}$.

(16) The OTTLE cell in the ECD spectrometer was connected to the electrochemical apparatus. When the potential reached a value corresponding to generation of either the radical-cation $[P\text{-}\mathbf{1}]^{\bullet+}$ (at −1.4 V) or the fully reduced form $[P\text{-}\mathbf{1}]^{0}$ (at −1.65 V), the potential scan was stopped, and the registration of ECD started. Electrolysis in the OTTLE cell leads to the complete conversion to the individual redox forms within a few seconds. This is confirmed from the fast time decay of the faradaic current. Hence the ECD spectra are not influenced by the time dependence of concentrations.

(17) All EPR spectroelectrochemical experiments were performed starting with $[P\text{-}\mathbf{1}]^{2+}$.

(18) Frisch, M. J.; Trucks, G. W.; Schlegel, H. B.; Scuseria, G. E.; Robb, M. A.; Cheeseman, J. R.; Scalmani, G.; Barone, V.; Mennucci, B.; Petersson, G. A.; Nakatsuji, H.; Caricato, M.; Li, X.; Hratchian, H. P.; Izmaylov, A. F.; Bloino, J.; Zheng, G.; Sonnenberg, J. L.; Hada, M.; Ehara, M.; Toyota, K.; Fukuda, R.; Hasegawa, J.; Ishida, M.; Nakajima, T.; Honda, Y.; Kitao, O.; Nakai, H.; Vreven, T.; Montgomery, J. A., Jr.; Peralta, J. E.; Ogliaro, F.; Bearpark, M.; Heyd, J. J.; Brothers, E.; Kudin, K. N.; Staroverov, V. N.; Kobayashi, R.; Normand, J.; Raghavachari, K.; Rendell, A.; Burant, J. C.; Iyengar, S. S.; Tomasi, J.; Cossi, M.; Rega, N.; Millam, N. J.; Klene, M.; Knox, J. E.; Cross, J. B.; Bakken, V.; Adamo, C.; Jaramillo, J.; Gomperts, R.; Stratmann, R. E.; Yazyev, O.; Austin, A. J.; Cammi, R.; Pomelli, C.; Ochterski, J. W.; Martin, R. L.; Morokuma, K.; Zakrzewski, V. G.; Voth, G. A.; Salvador, P.; Dannenberg, J. J.; Dapprich, S.; Daniels, A. D.; Farkas, Ö.; Foresman, J. B.; Ortiz, J. V.; Cioslowski, J.; Fox, D. J. *Gaussian 09*, Revision D.01; Gaussian, Inc.: Wallingford, CT, 2013.

(19) (a) Zheng, X.; Wang, X.; Qiu, Y.; Li, Y.; Zhou, C.; Sui, Y.; Li, Y.; Ma, J.; Wang, X. *J. Am. Chem. Soc.* **2013**, *135*, 14912. (b) Porter, W. W., III; Vaid, T. P.; Rheingold, A. L. *J. Am. Chem. Soc.* **2005**, *127*, 16559.

(20) The only discrepancy is the appearance of negative band of $[P\text{-}\mathbf{1}]^{0}$ at 369 nm in the theoretical spectra (Figure 5C). We believe that this theoretical transition vanishes in the positive band at 314 nm which appears towards longer wavelengths in experiment.

(21) [6]Helicene system **3** has $\Delta(\Delta\varepsilon)$ value of −45 M^{-1} cm^{-1} at 340 nm, see ref 6. See also ref 8a for interconversion of an axially chiral biaryl into a helicenoid with $\Delta(\Delta\varepsilon)$ value of 140 M^{-1} cm^{-1} at 290 nm.

(22) For combination of axially chiral scaffolds with electrochromic units: (a) Deng, J.; et al. *Org. Lett.* **2007**, *9*, 5393. (b) Hasegawa, M.; et al. *Org. Lett.* **2011**, *13*, 4688. (c) Beer, G.; et al. *Angew. Chem., Int. Ed.* **2000**, *39*, 3252.

(23) Zhang, G.; Zhang, D.; Zhu, D. In *Electrochemistry of Functional Supramolecular Systems*; Ceroni, P., Credi, A., Venturi, M., Eds.; Wiley: Hoboken, NJ, 2010; pp 447−476.

(24) (a) Avarvari, N.; Wallis, J. D. *J. Mater. Chem.* **2009**, *19*, 4061. (b) Pop, F.; Auban-Senzier, P.; Frackowiak, A.; Ptaszynski, K.; Olejniczak, I.; Wallis, J. D.; Canadell, E.; Avarvari, N. *J. Am. Chem. Soc.* **2013**, *135*, 17176.